THE JOURNAL OF PHYSICAL CHEMISTRY B LETTERS

2005, *109,* 44−47
Published on Web 12/17/2004

Characterization of Molybdenum Carbide Nanoparticles Formed on Au(111) Using Reactive-Layer Assisted Deposition

Jillian M. Horn,[†,‡] Zhen Song,[†] Denis V. Potapenko,[†] Jan Hrbek,[†] and Michael G. White*[,†,‡]

Chemistry Department, Brookhaven National Laboratory, Upton, New York 11973, and Department of Chemistry, SUNY Stony Brook, Stony Brook, New York 11794

Received: November 10, 2004; In Final Form: November 30, 2004

Temperature programmed desorption (TPD), Auger electron spectroscopy (AES), X-ray photoelectron spectroscopy (XPS), and scanning tunneling microscopy (STM) have been used to characterize molybdenum carbide nanoparticles prepared on a Au(111) substrate. The MoC_x nanoparticles were formed by Mo metal deposition onto a reactive multilayer of ethylene, which was physisorbed on a Au(111) substrate at low temperatures (<100 K). The resulting clusters have an average diameter of ∼1.5 nm and aggregate in the fcc troughs located on either side of the elbows of the reconstructed Au(111) surface. Core level XPS shows that the electronic environment of the Mo and C atoms in the nanoparticles is similar to that found in Mo_2C-(0001) single crystals and carburized Mo metal surfaces. Peak intensities in XPS and AES spectra were used to estimate an average Mo/C atomic ratio of 1.2 ± 0.3 for nanoparticles annealed above 600 K.

Introduction

The early transition metal carbides have received considerable interest due to their potential as catalysts for a wide range of heterogeneous reactions.[1−3] In many cases, the metal carbides offer advantages of selectivity and resistance to poisoning over the parent metal, and for certain reactions their catalytic behavior is similar to that of the group 8−10 noble metals.[1−6] One of the most actively studied systems is molybdenum carbide, which has been shown to be a very active catalyst for methane reforming,[7,8] aromatization,[9,10] dehydrogenation,[6,11,12] and hydrodesulfurization (HDS).[13−16] In model HDS studies, molybdenum carbide was found to be more active than MoS_2 surfaces[15,16] and the Ni-promoted MoS_2 commercial catalyst.[14] The higher activity of molybdenum carbide correlates with increased electron density near the Fermi level.[15−17]

The stoichiometry of bulk molybdenum carbide is Mo_2C, although the phase diagram exhibits a wide range of Mo/C stoichiometry, including MoC (1:1) phases with hexagonal (γ-MoC, η-MoC) and cubic (δ-MoC) structures.[18] Surfaces of the carbide can be carbon or metal terminated, and nonstoichiometric Mo/C ratios are often observed on carburized Mo surfaces that exhibit reactivity that is strongly dependent on the surface composition and annealing temperature.[19−21] Nanoparticles of molybdenum carbide offer the possibility of creating a wider variation in surface structure and composition, which could result in further modification of catalytic activity and selectivity. For example, Suslick and co-workers recently demonstrated the sonochemical synthesis of molybdenum carbide nanoparticles (∼2 nm) that exhibited dehydrogenation activity that was comparable to a dispersed Pt catalyst.[22]

The most common preparation method of molybdenum carbide surfaces is by the thermal cracking of ethylene on a molybdenum metal surface at high temperatures.[15,19] In principle, this approach should also be effective for carbiding bare Mo nanoparticles, which can be prepared by simple physical vapor deposition (PVD) of Mo atoms on the reconstructed Au(111) surface.[23−25] Very recent studies have shown, however, that Mo deposited on Au(111) is spontaneously encapsulated by Au atoms at temperatures above 300 K.[26,27] Not surprisingly, the gold encapsulated Mo nanoparticles are less reactive toward most adsorbates, making it virtually impossible to carbide the Mo particles by exposure to simple carbon containing molecules (ethylene, butadiene) at temperatures below which the herringbone structure of the Au(111) substrate is stable (<800 K).[26]

In this work, we report on a novel process for the preparation of MoC_x nanoparticles, which involves the deposition of Mo atoms onto multilayers of ethylene condensed onto a Au(111) substrate at temperatures below 100 K. This approach builds on earlier methods involving co-deposition of evaporated metal atoms and gas-phase reactants,[23,28] and the use of low temperature, rare gas thin films for modifying metal nanoparticle growth and morphology (buffer-layer assisted growth).[29−31] The use of reactive multilayers was demonstrated very recently in a study of nanoscale MgO films prepared by Mg atom deposition on O_2 multilayers at 22 K.[32] Here, we show that the reaction of "hot" Mo atoms with the ethylene overlayer results in the formation of MoC_x nanoparticles ($x \approx 1$) with electronic character similar to that of the bulk carbide. By analogy with earlier work,[29−31] we call this method reactive-layer assisted deposition (RLAD) and expect it to be very useful for preparing a wide range of supported nanoparticles of transition metal carbides, nitrides, oxides and sulfides.

* Corresponding author. E-mail: mgwhite@bnl.gov. Ph: (631) 344-4345. Fax: (631) 344-5815.
† Brookhaven National Laboratory.
‡ SUNY Stony Brook.

10.1021/jp044837i CCC: $30.25

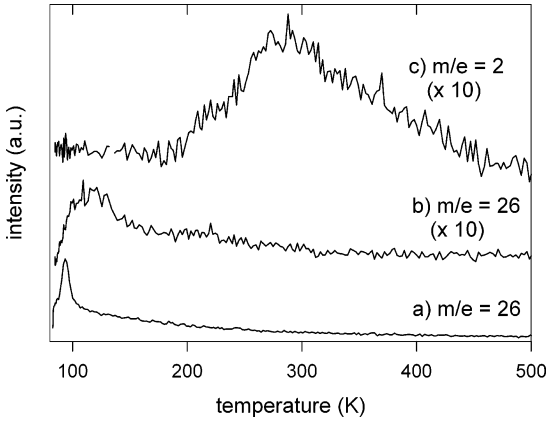

Figure 1. Thermal desorption spectra of 180 langmuir ethylene on Au(111): (a) with no deposited Mo; (b, c) after Mo deposition.

Experimental Section

The STM experiments were carried out in an ultrahigh vacuum system equipped with a variable temperature scanning tunneling microscope (Omicron). A preparation chamber equipped with a LEED/Auger, mass spectrometer, and e-beam evaporator was used for sample cleaning and preparation. The Au(111) surface was cleaned by cycles of Ne^+ sputtering (1 keV) at room temperature, followed by annealing to 900 K. The Au samples were determined to be clean when the STM images showed extended domains of the herringbone reconstruction, or when no impurities were detected by XPS or AES. The XPS experiments were performed in a UHV surface science chamber, which is a part of the U7A beam line located at the National Synchrotron Light Source at Brookhaven National Laboratory. This chamber is equipped with a hemispherical electron energy analyzer with multichannel detection. The Mo 3d, C 1s, Au 4f, and valence band spectra were recorded at a photon energy of 380 eV. The binding energy scale in the photoemission data was calibrated to the position of the Fermi edge and the Au 4f peaks. TPD and AES measurements were completed in another UHV chamber, equipped with a quadrupole mass spectrometer, Auger spectrometer, and a metal evaporation source.

Results and Discussion

Thermal desorption experiments were performed to monitor the formation of MoC_x particles synthesized by Mo deposition on ethylene/Au(111). Figure 1 shows TPD results during MoC_x formation for a 180 langmuir exposure of ethylene, as compared to ethylene on bare Au(111). Ethylene on Au(111) shows a single molecular desorption peak at 93 K. No H_2 desorption could be detected, indicating that ethylene desorbs from Au(111) without decomposition. This is consistent with previous studies of physisorbed ethylene on Ag(111)[33] and Ag(100),[34] where only molecular desorption is observed below 105 K. When Mo has been deposited on the ethylene/Au(111) surface, the ethylene desorption peak is seen to shift to higher temperatures and extend over a wider temperature range (100 to 170 K). The change in desorption is attributed to the presence of Mo on the surface. Hydrogen desorption is observed between 200 and 425 K, which is typical of hydrogen recombinative desorption from Mo particles on Au(111)[26] and indicative of ethylene and ethylene fragments (C_xH_y) reacting on bare and carbided Mo surfaces. Auger electron spectroscopy (AES) confirms the presence of carbon after annealing the surface to 600 K. Variation of the thickness of the ethylene overlayer did not significantly alter the relative intensity of the Mo and C AES peaks.

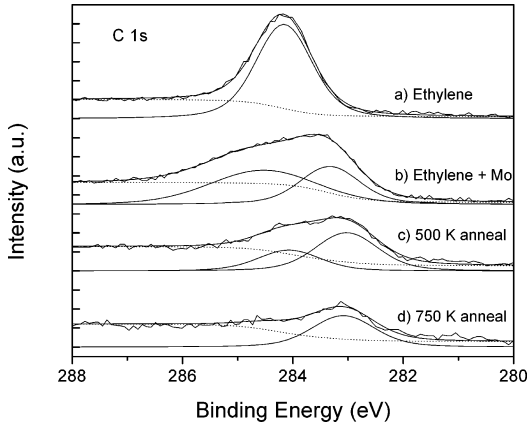

Figure 2. C 1s photoemission spectra: (a) ethylene on Au(111); (b) after Mo deposition on the ethylene layer at 100 K; (c, d) subsequent annealing to higher temperatures. A Levenberg−Marquardt method for nonlinear least-squares fit was used with the fitted data shown. Prior to fitting, a Shirley-type background was subtracted, as shown by the dashed lines.

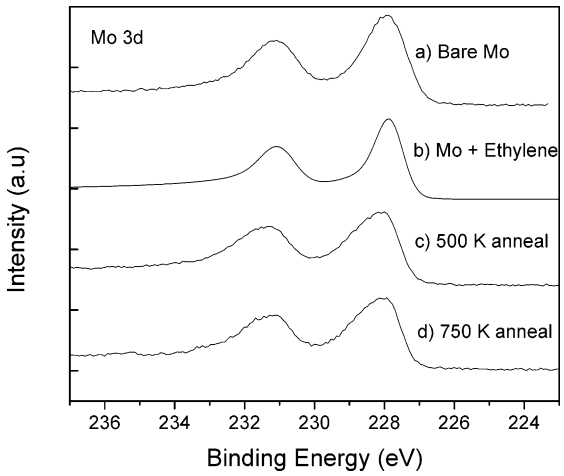

Figure 3. Mo 3d photoemission spectra: (a) bare Mo deposited at 100 K; (b) Mo deposited on an ethylene layer; (c, d) after subsequent annealing.

Mo 3d and C 1s photoemission spectra of the MoC_x clusters with subsequent annealing are shown in Figures 2 and 3, respectively. These spectra represent a Mo coverage of approximately 0.75 monolayer as calibrated in a previous study of Mo deposition on Au(111).[26] Spectra of the ethylene/Au(111) surface before Mo deposition show a single C 1s peak at 284.1 eV. This binding energy is consistent with the C 1s peak of weakly bound ethylene on other surfaces.[35] Upon Mo deposition at 100 K, two peaks are present in the C 1s spectrum, and both are shifted with respect to the ethylene peak. Consistent with the binding energy of carbon for a $Mo_2C(0001)$ single crystal,[21,36,37] we attribute the peak observed at 283.3 eV to molybdenum carbide. This peak shifts slightly to a lower binding energy (283.1 eV) upon annealing above 300 K. Similar shifts with annealing have been seen on molybdenum carbide thin films and could be explained by a coordination change of the carbon atoms.[20] In addition, a wide peak is seen in the range 284.0−284.5 eV, which we tentatively assign to hydrocarbon fragments on the surface.[15] The hydrocarbon peak diminishes with higher annealing temperatures and completely disappears when annealed to 750 K.

Photoemission spectra for the Mo $3d_{5/2}$ and $3d_{3/2}$ levels of MoC_x nanoparticles annealed above 500 K (Figure 3c,d) show asymmetric broadening and slight shifts in binding energies

relative to bare Mo particles (Figure 3a) or MoC_x species (Figure 3b) formed at low temperature. We attribute the asymmetric peak shapes to variations in the Mo electronic environment resulting from particles of different sizes and Mo/C atomic compositions. The $3d_{5/2}$ and $3d_{3/2}$ peak binding energies for the annealed MoC_x particles are 227.7 and 231.0 eV, respectively. These values are only slightly lower (∼0.2 eV) than that for the Mo metal[15] and very close to that reported for the Mo_2C-(0001) single crystal[36−38] and carburized Mo surfaces.[15,16,21]

The average composition of the MoC_x particles was estimated from AES and XPS peak intensities for molybdenum and carbon. The AES carbon (275 eV) and molybdenum (190 eV) peak heights for MoC_x/Au(111) particles annealed to 600 K were calibrated against a bulk Mo_2C (Alfa Aesar) sample. XPS peak intensities of the Mo 3d and carbidic C 1s (283.3 eV) peaks were also used to estimate the composition of MoC_x nanoparticles. Here, the integrated peak intensities obtained from least-squares fits of photoemission spectra (see Figure 2) were normalized using the C 1s and Mo 3d photoionization cross sections.[39] The combined AES and XPS measurements (averaged over six MoC_x/Au(111) surface preparations) yield a Mo/C ratio that increases from 1.0 ± 0.2 for surfaces annealed at 600 K to a value of 1.3 ± 0.3 for higher annealing temperatures (750−800 K). Assuming a uniform composition, a Mo/C ratio of approximately 1:1 suggests that the particles are similar in structure to the stable γ-MoC phase.[18] The increase in the Mo/C ratio with increasing annealing temperature, however, is typical of carbon rich surfaces formed by carburization of Mo metal.[1,19−21] For the latter, an increasing Mo/C AES ratio with high-temperature annealing (600−1300 K) was ascribed to the dissolution of surface carbon into the bulk and the short escape depth (∼1 nm) of the emitted Auger electrons. The XPS and AES experiments in this work detect electrons over a similar kinetic energy range (100−300 eV) with escape depths that are expected to be comparable to the MoC_x nanoparticle thickness (≤1 nm from STM images discussed below). Preferential detection of surface atoms is nonetheless expected, and the temperature dependent Mo/C ratio is most likely a reflection of changes in the surface composition of the particles. Further evolution of the Mo/C surface composition could be expected at higher annealing temperatures (>1000 K); however, the surface structure of the Au(111) substrate is not stable above 800 K.[26]

An STM image of MoC_x nanoparticles prepared on Au(111) at 100 K and warmed to room temperature is shown in Figure 4a. The Mo coverage used for the STM experiments (0.1 monolayer) is much smaller than in the XPS and TPD experiments (0.75 to 1.0 monolayer) to clearly image individual clusters. It is seen in Figure 4a that the RLAD method produces nanoparticles of uniform size, with diameters of approximately 1.5 nm. The size distribution, given as cluster area (nm^2) assuming a circular cross section, is shown in Figure 4c. Interestingly, the MoC_x clusters are observed to preferentially nucleate on either side of the "elbow" dislocation of the herringbone reconstruction, in the fcc stacking regions. By contrast, bare Mo nanoparticles deposited by PVD nucleate at the elbows of the herringbone structure.[23,26] This is shown in Figure 4b, where Mo was deposited on the bare Au(111) surface at the same temperature and coverage as in Figure 4a. In addition to nucleating primarily at the elbow sites, the Mo particles are larger, as shown in Figure 4c.

STM images taken after annealing to higher temperatures did not show significant changes in particle morphology, as compared to Figure 4a, although distortion of the Au(111) herringbone structure and Au atom migration were evident at the highest temperatures investigated (750 K). Atom diffusion leads to the formation of small Au(111) islands upon which some MoC_x nanoparticles reside. In contrast, annealing of bare Mo/Au(111) surfaces leads to the formation of etching "pits" along the Au(111) step edges, indicative of Au atom consumption.[26,40] We have recently shown that the Au atoms removed from the step edges diffuse to and encapsulate the Mo particles.[26]

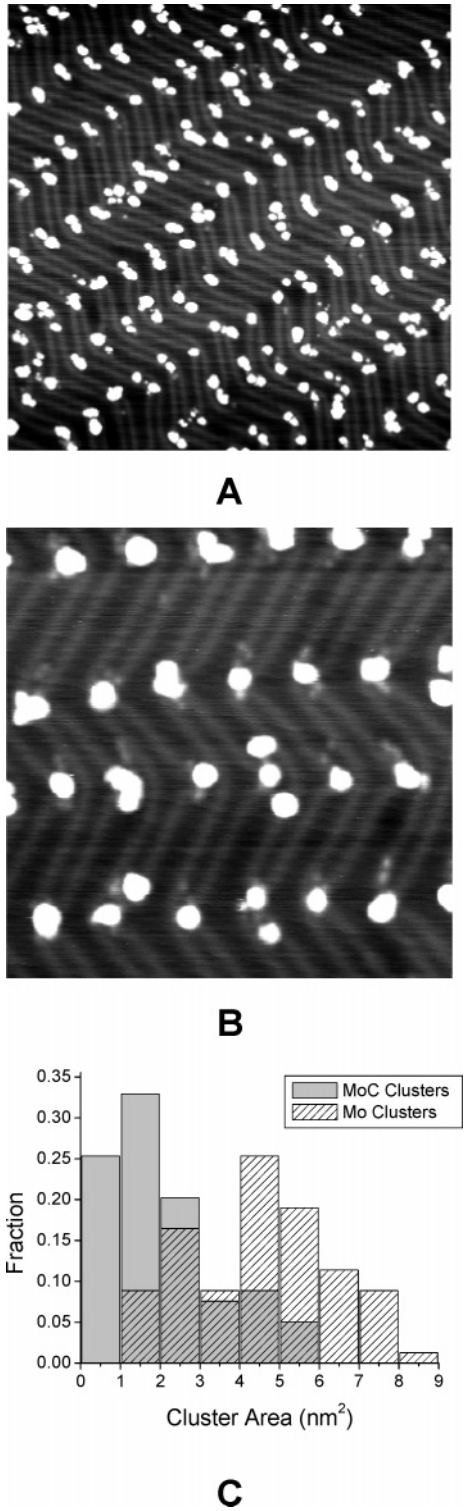

Figure 4. STM images: (A) MoC_x with approximately 0.1 monolayer Mo deposited by RLAD (image size: 100 × 100 nm^2); (B) Mo clusters deposited by PVD (0.1 monolayer) (image size: 50 × 50 nm^2); (C) cluster size distributions of MoC_x and Mo clusters.

The lack of such features in the STM images for MoC_x/Au(111) particles at higher temperatures suggests that they are not capped by Au atoms. The differences observed in morphology, nucleation, and annealing following Mo deposition on bare and ethylene covered Au(111) surfaces provide further evidence that MoC_x nanoparticles are formed by the RLAD method.

Summary

We have demonstrated the formation of MoC_x nanoparticles using reactive-layer assisted deposition (RLAD) in which Mo atoms are deposited onto ethylene multilayers prepared on a Au(111) substrate at low temperatures. This approach results in a narrow distribution of nanoclusters of MoC_x that are stable against high-temperature annealing. TPD, AES, and XPS experiments were used to monitor and confirm the formation of molybdenum carbide particles, with an average Mo/C atomic ratio of 1.2 ± 0.3 for surfaces annealed above 600 K. STM images show cluster morphology that is different from that of bare Mo clusters deposited by PVD, with the clusters preferentially located in the fcc troughs on either side of the "elbows" of the herringbone reconstruction. Current studies are underway to probe the reactivity of the MoC_x/Au(111) nanoparticles.

Acknowledgment. We thank Dr. J. Rodriguez and Dr. X. Zhao for valuable assistance at the U7A beamline at the NSLS. This research was carried out at Brookhaven National Laboratory under contract DE-AC02-98CH10086 with the U.S. Department of Energy (Division of Chemical Sciences).

References and Notes

(1) Chen, J. G. *Chem. Rev.* **1996**, *96*, 1477 and references therein.
(2) Oyama, S. T. *Catal. Today* **1992**, *15*, 179 and references therein.
(3) Oyama, S. T. Introduction to the chemistry of transition metal carbides and nitrides. In *The Chemistry of Transition Metal Carbides and Nitrides*; Oyama, S. T., Ed.; Blackie Academic: Glasgow, 1996; pp 1 and references therein.
(4) Levy, R. L.; Boudart, M. *Science* **1973**, *181*, 547.
(5) Eberhardt, M. E.; MacLaren, J. M. The origins of the similarities between the late transition metals and early transition metal monocarbides. In *The Chemistry of Transition Metal Carbides and Nitrides*; Oyama, S. T., Ed.; Blackie Academic: Glasgow, 1996; pp 107.
(6) Fruhberger, B.; Chen, J. G. *J. Am. Chem. Soc.* **1996**, *118*, 11599.
(7) Claridge, J. B.; York, A. P. E.; Brungs, A. J.; Marquez-Alvarez, C.; Sloan, J.; Tsang, S. C.; Green, M. L. H. *J. Catal.* **1998**, *180*, 85.
(8) Xiao, T. C.; Hanif, A.; York, A. P. E.; Nishizaka, Y.; Green, M. L. H. *Phys. Chem. Chem. Phys.* **2002**, *4*, 4549.
(9) Solymosi, F.; Cserenyi, J.; Szoke, A.; Bansagi, T.; Oszko, A. *J. Catal.* **1997**, *165*, 150.
(10) Solymosi, F.; Szechenyi, A. *J. Catal.* **2004**, *223*, 221.
(11) Liu, N.; Rykov, S. A.; Chen, J. G. *Surf. Sci.* **2001**, *487*, 107.
(12) Fruhburger, B.; Chen, J. G. *Surf. Sci.* **1996**, *367*, L102.
(13) Sajkowski, D. J.; Oyama, S. T. *Appl. Catal. A* **1996**, *134*, 339.
(14) Aegerter, P. A.; Quigley, W. W. C.; Simpson, G. J.; Ziegler, D.; Logan, J. W.; McCrea, K. R.; Glazier, S.; Busell, M. E. *J. Catal.* **1996**, *164*, 109 and references therein.
(15) Rodriguez, J. A.; Dvorak, J.; Jirsak, T. *Surf. Sci.* **2000**, *457*, L413.
(16) Rodriguez, J. A.; Dvorak, J.; Jirsak, T. *J. Phys. Chem. B* **2000**, *104*, 11515.
(17) Liu, P.; Rodriguez, J. A. *J. Chem. Phys.* **2004**, *120*, 5414.
(18) Hugosson, H. W.; Eriksson, O.; Nordstrom, L.; Jansson, U.; Fast, L.; Delin, A.; Willis, J. M.; Johansson, B. *J. Appl. Phys.* **1999**, *86*, 3758 and references therein.
(19) Fruhberger, B.; Chen, J. G. *Surf. Sci.* **1995**, *342*, 38.
(20) Fruhberger, B.; Chen, J. G.; Eng, J.; Bent, B. E. *J. Vac. Sci. Technol. A* **1996**, *14*, 1475.
(21) Reinke, P.; Oelhafen, P. *Surf. Sci.* **2000**, *468*, 203.
(22) Hyeon, T.; Fang, M.; Suslick, K. S. *J. Am. Chem. Soc.* **1996**, *118*, 5492.
(23) Helveg, S.; Lauritsen, J. V.; Laegsgaard, E.; Stensgaard, I.; Norskov, J. K.; Clausen, B. S.; Topsoe, H.; Besenbacher, F. *Phys. Rev. Lett.* **2000**, *84*, 951.
(24) Song, Z.; Cai, T.; Rodriguez, J. A.; Hrbek, J.; Chan, A. S. Y.; Friend, C. M. *J. Phys. Chem. B* **2003**, *107*, 1036.
(25) Rodriguez, J. A.; Dvorak, J.; Jirsak, T.; Hrbek, J. *Surf. Sci.* **2001**, *490*, 315.
(26) Potapenko, D. V.; Horn, J. M.; Beuhler, R. J.; Song, Z.; White, M. G. *Surf. Sci.*, in press.
(27) Liu, P.; Rodriguez, J. A.; Muckerman, J. T.; Hrbek, J. *Phys. Rev. B* **2003**, *67*, 155416.
(28) Bollinger, M. V.; Lauritsen, J. V.; Jacobsen, K. W.; Norskov, J. K.; Helveg, S.; Besenbacher, F. *Phys. Rev. Lett.* **2001**, *87*, 196803.
(29) Huang, L.; Chey, S. J.; Weaver, J. H. *Phys. Rev. Lett.* **1998**, *80*, 4095.
(30) Antonov, V. N.; Palmer, J. S.; Bhatti, A. S.; Weaver, J. H. *Phys. Rev. B* **2003**, *68*, 205418.
(31) Kerner, G.; Asscher, M. *Nano Lett.* **2004**, *4*, 1433.
(32) Kim, J.; Dohnalek, Z.; White, J. M.; Kay, B. D. *J. Phys. Chem. B* **2004**, *108*, 11666.
(33) Felter, T. E.; Weinberg, W. H.; Zhdan, P. A.; Boreskov, G. K. *Surf. Sci. Lett.* **1980**, *97*, L313.
(34) Vattuone, L.; Savio, L.; Rocca, M.; Rumiz, L.; Baraldi, A.; Lizzit, S.; Comelli, G. *Phys. Rev. B* **2002**, *66*, 085403.
(35) Rochet, F.; Jolly, F.; Bournel, F.; Dufour, G.; Sirotti, F.; Cantin, J. L. *Phys. Rev. B* **1998**, *58*, 11029.
(36) St. Clair, T. P.; Oyama, S. T.; Cox, D. F.; Otani, S.; Ishizawa, Y.; Lo, R.; Fukui, K.; Iwasawa, Y. *Surf. Sci.* **1999**, *426*, 187.
(37) Sugihara, M.; Ozawa, K.; Edamoto, K.; Otani, S. *Solid State Commun.* **2002**, *121*, 1.
(38) St. Clair, T. P.; Oyama, S. T.; Cox, D. F. *Surf. Sci.* **2002**, *511*, 294.
(39) Yeh, J. J.; Lindau, I. *At. Data Nucl. Data Tables* **1985**, *32*, 1.
(40) Altman, E. I.; Colton, R. J. *Surf. Sci. Lett.* **1994**, *304*, L400.